RSC Advances

PAPER

View Article Online
View Journal | View Issue

Cite this: *RSC Adv.*, 2026, **16**, 26127

Pyrolysis-assisted catalytic conversion of wood in hot-compressed water for the production of aromatic monomers and syngas without external hydrogen addition

Alex Ikeda-Francisco, Jiaqi Wang, Eiji Minami and Haruo Kawamoto *

Efficient conversion of lignocellulosic biomass into value-added chemicals is essential for sustainable chemistry. Japanese cedar and Japanese beech were treated in hot-compressed water (300–450 °C) with Pd/C, yielding aromatic monomers and syngas without external hydrogen. Polysaccharides were hydrolyzed to monosaccharides, fragmented to syngas, and provided hydrogen *via* the water-gas-shift reaction. This *in situ* hydrogen stabilized lignin-derived aromatic monomers through hydrogenation of aliphatic C_α=C_β bonds, preventing repolymerization and enabling bond cleavage for high yields. At lower temperatures, guaiacols and syringols dominated, with Japanese beech producing a more complex mixture. Above 400 °C, both woods yielded primarily catechols and phenols, and species-specific differences disappeared. At 450 °C, however, hydrogenation of aromatic rings occurred as a side reaction, reducing selectivity. Water-soluble intermediates from polysaccharides temporarily suppressed catalyst activity but were gasified to restore efficiency. These results highlight a promising biomass-based route to aromatic monomers and syngas as sustainable alternatives to petroleum-derived processes.

Received 3rd February 2026
Accepted 8th April 2026

DOI: 10.1039/d6ra00940a

rsc.li/rsc-advances

Introduction

Wood is a promising renewable alternative to petroleum for sourcing both aliphatic and aromatic carbons. The cellulose and hemicellulose fractions of wood, which account for approximately 65–80% of its composition, can be converted to syngas (CO + H_2) by gasification. This makes wood polysaccharides an attractive renewable source of hydrogen, especially given that 99% of the global hydrogen supply is currently derived from fossil fuels without carbon capture.[1] Syngas serves as a precursor for synthetic hydrocarbons *via* Fischer–Tropsch reactions. Meanwhile, lignin, comprising 20–35% of wood, can be transformed into industrially important aromatic monomers such as phenols and BTX compounds (benzene, toluene and xylene). Therefore, the components of wood offer strategic potential for defossilizing the chemical industry, which remains heavily dependent on fossil-based feedstocks for chemical manufacturing.[2–4]

Syngas and hydrogen production from wood has been extensively studied through gasification and hydrothermal gasification processes. Conventional gasification is typically carried out at high temperatures ranging from 700 to 1000 °C, and steam-blown gasification promotes the conversion of CO to H_2 *via* the water-gas shift reaction.[5] However, the practical application of this method faces significant challenges, particularly the formation of tar, which can cause clogging of pipelines.[6] In contrast, hydrothermal gasification enables hydrogen production under high-pressure conditions at relatively lower temperatures (350–650 °C),[7] and active research is ongoing in the development of efficient catalysts for this process.[8] Additionally, lignin-derived compounds are also being targeted for gasification, primarily through hydrogenation of the aromatic rings followed by gasification.

The production of aromatic monomers from lignin has been extensively studied through pyrolysis and catalytic conversion. Fast pyrolysis is a widely explored method for obtaining high yields of condensable volatile products, facilitating the recovery of lignin-derived aromatics.[9] However, monomer yields remain low, with the process primarily generating dimers and higher molecular weight oligomers.[10,11] This is largely attributed to the stability of C–C linkages in condensed structures and the pronounced re-polymerization of pyrolysis intermediates *via* radical coupling and quinone methide mechanisms during pyrolysis.[10,12,13] Ether bonds within the lignin structure typically cleave through homolytic mechanisms, generating products containing conjugated C=C double bonds, which readily undergo re-polymerization through quinone methide intermediates.

To overcome these challenges, various studies have investigated the thermal degradation of lignocellulosic substrates over

Department of Socio-Environmental Energy Science, Graduate School of Energy Science, Kyoto University, Yoshida-honmachi, Sakyo-ku, Kyoto 606-8501, Japan. E-mail: kawamoto@energy.kyoto-u.ac.jp

noble metal catalysts in various solvents.[14–17] Most of these studies were conducted at temperatures below 250 °C [17,18] in order to preserve the carbohydrate fraction (the so-called "lignin-first" process). However, under such conditions, the monomer yields are generally low, particularly for softwood lignin.

In our previous work,[19,20] we demonstrated that catalytic hydrogenolysis at elevated temperatures above 250 °C—preferably above 300 °C—in various solvents such as aromatic solvents could effectively suppress repolymerization of pyrolysis intermediates. This approach not only inhibited recondensation reactions but also enabled the hydrogenolytic cleavage of thermally stable condensed lignin structures, resulting in aromatic monomer yields exceeding 60 mol% (based on the aromatic rings of lignin) from softwood lignin.[19,20] Building on this strategy, the present study explores catalytic hydrogenolysis in hot-compressed water as a means to simultaneously produce hydrogen and aromatic monomers. Unlike the conventional lignin-first process, which requires external hydrogen input or hydrogen-donating agents (*e.g.*, primary alcohols) to retain polysaccharides,[21–23] our approach leverages the gasification of the carbohydrate fraction to provide the necessary hydrogen, thereby eliminating the need for external hydrogen sources.

One reason why softwood lignin is more difficult to depolymerize than hardwood lignin is the higher proportion of condensed (C–C) structures resulting from differences in aromatic unit composition. Softwood lignin consists exclusively of guaiacyl (4-hydroxy-3-methoxyphenyl, G) units, which can form condensed linkages through the 5-position. In contrast, hardwood lignin contains both G units and syringyl (3,5-dimethoxy-4-hydroxyphenyl, S) units, the latter bearing a methoxy group at the 5-position that prevents condensation, thereby reducing the fraction of condensed structures. However, a drawback of hardwood lignin is the greater complexity in the composition of the resulting aromatic monomers due to the coexistence of both G and S units. Given these structural and compositional differences in lignin reactivity, this study employed Japanese cedar (*Cryptomeria japonica*, a softwood) and Japanese beech (*Fagus crenata*, a hardwood) as model feedstocks.

In this paper, Japanese cedar and Japanese beech were treated in hot-compressed water in the temperature range of 300–450 °C under a N_2 atmosphere, and the formation behaviors of syngas and aromatic monomers were investigated and compared between the two species. In addition, studies using model compounds were conducted to further discuss the conversion mechanisms of the individual components as well as the effects on catalytic transformations.

Results and discussion

Japanese beech and Japanese cedar wood flours were dispersed in water with Pd/C and treated in a batch reactor under a nitrogen atmosphere at 300–450 °C for 60 min (Fig. S1). The resulting mixtures were separated into gas, water-soluble, EtOAc-soluble, and solid char fractions (Fig. S2). The soluble fractions were evaporated and weighed after no visible solvent remained, while the char fraction was collected directly as the solid residue and weighed after drying. The yields, expressed on a dry weight basis of wood (wt%), are shown in Fig. 1. Additional data on different reaction durations (5, 15 and 30 min) at 350 °C and 450 °C for both wood types are provided in the SI (Table S1, Fig. S3 and S4). The overall recovery was high (55.8–93.3 wt%), which is notable given that volatile products, including water, were not included in the quantification. In addition, losses due to gas diffusion through the thin polypropylene gas bag during the gas analysis step may have contributed to the lower observed yields.

The yield of the water-soluble fraction ranged from 0.3 to 13.9 wt% —not high but consistently present across all conditions. Yields of water-soluble products were higher at shorter reaction times (5–30 min) at 350 °C (Fig. S3), but not at 400 °C (Fig. S4), suggesting that the degradation of water-soluble products was accelerated under more severe conditions. Since these products were not detected in the MWL experiments, they are presumed to originate from wood polysaccharides. Although the water-soluble fraction was also produced from Avicel, its yield under similar conditions was lower than that from wood. As discussed later, the water-soluble fraction is considered a by-product of polysaccharide gasification.

In the MWL experiments, the yield of the EtOAc-soluble fraction was high, while the gas yield was relatively low at about 15 wt%. In contrast, the amount of the EtOAc-soluble fraction from Avicel was negligible. These results indicate that the EtOAc-soluble fraction originates mainly from lignin-derived products.

The compositions of the EtOAc-soluble fraction and the gaseous products were analyzed by GC-MS and Micro GC, respectively, with the results shown in Fig. 2. Yields obtained at 350 °C and 400 °C for various reaction times (5, 15, 30 and 60 min) from both wood types are summarized in Fig. S5 and S6, respectively. Yields at 450 °C for reaction times of 5 and 60 min are shown in Fig. S7. Aromatic monomers derived from lignin are expressed as mol% relative to the benzene-ring content of lignin in the wood. Since the gaseous products were suggested to originate from wood polysaccharides, gas yields are expressed as carbon-based mol% relative to the polysaccharide content. Additionally, since hydrogen is not included in the carbon-based yields, the molar proportions of all gaseous components, including hydrogen, are also presented.

Lignin-derived aromatic monomers

Lignin-derived aromatic monomers were characterized by saturated methyl, ethyl, propyl, or hydrogen substituents at the para-position to the phenolic –OH. In terms of aromatic nuclei, products from Japanese cedar (softwood) contained mainly guaiacyl (G) units, while those from Japanese beech (hardwood) contained both G and syringyl (S) units at lower temperatures. As the treatment temperature increased, demethoxylation and demethylation of methoxy groups progressed, leading to higher proportions of phenol and catechol units. Remarkably, at 400 °C, high yields were maintained (68.9 mol% for beech and

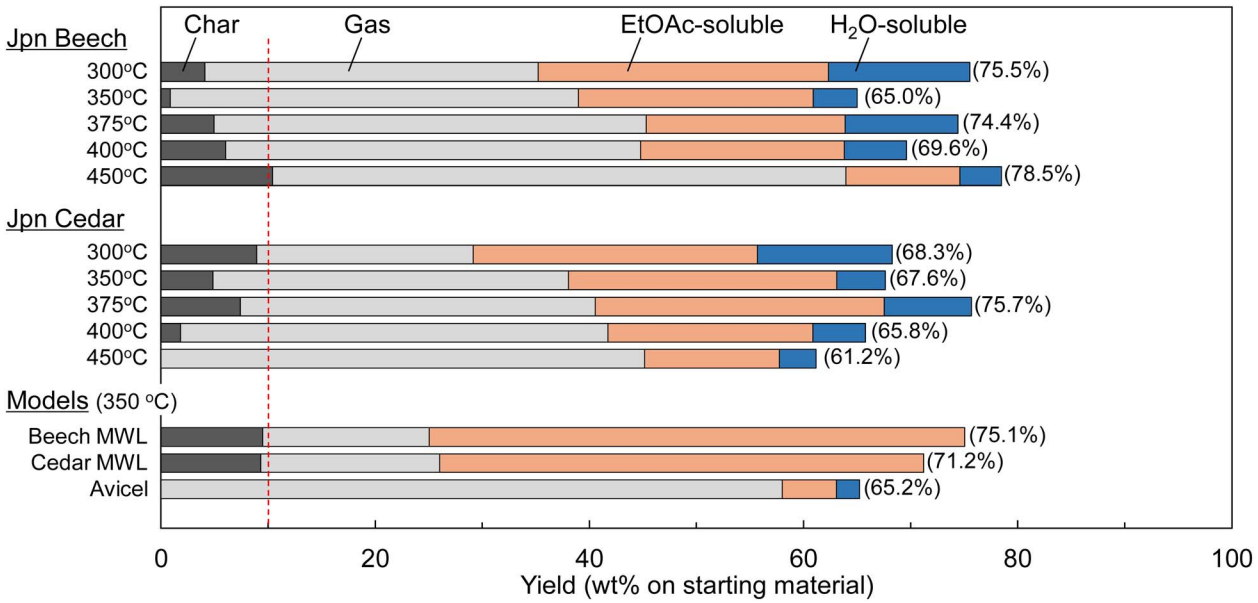

Fig. 1 Yields of char, gas, EtOAc-soluble and water-soluble products from Japanese beech and Japanese cedar (100 mg) and from isolated lignin and cellulose samples (25–100 mg), treated at various temperatures for 60 min in H_2O (1 mL) under N_2 (1 atm, prior to heating) over Pd/C (25 mg). Values in parentheses indicate the total yield of the products.

59.5 mol% for cedar), but the aromatic monomers consisted predominantly of catechols and phenols, and the compositional differences between cedar and beech disappeared. This simplification of aromatic monomer composition is advantageous for producing aromatic monomers from hardwood. In contrast, the alkyl side-chain composition showed little change, indicating that side-chain transformations are not significant below 450 °C.

As discussed later, the S units of Japanese beech were gradually converted from S → G → catechol → phenol units, and a small amount of methoxycatechol units was also detected, formed by demethylation of methoxy groups. This transition is more clearly observed by comparing the monomer compositions obtained at different reaction times at 400 °C (Fig. S6). In contrast, pyrogallol units, in which both methoxy groups are replaced by –OH, were not observed. Possible pathways such as methoxycatechol → G units *via* dehydroxylation and pyrogallol → catechol units *via* dehydroxylation may exist, but further investigation is required.

A comparison of aromatic monomer yields from Japanese beech and Japanese cedar revealed clear differences. Under the 60 min treatment conditions (Fig. 2), Japanese beech consistently produced high yields—above approximately 70 mol%—across 300–400 °C range. In contrast, Japanese cedar showed lower yields (42.8 mol% at 300 °C), which increased with temperature, reaching 59.5 mol% at 400 °C. A similar trend was observed when varying the treatment duration at 350 °C (Fig. S5) and 400 °C (Fig. S6). For Japanese beech, the monomer yield at 350 °C increased rapidly from 43.0 mol% (5 min) and 44.6 mol% (15 min) to 76.1 mol% (30 min) and 70.0 mol% (60 min), indicating that most monomer formation was completed within 30 min. Yields at 400 °C remained consistently high across all durations (66.7–74.3 mol%). In contrast, Japanese cedar showed a steady increase in monomer yield with reaction time at both 350 and 400 °C, suggesting that monomer formation progressed more gradually and continued even at 60 min. This indicates that Japanese beech undergoes faster monomer release than Japanese cedar under the same conditions.

This difference can be explained by structural variations in lignin between hardwoods and softwoods. In softwoods, G units lack a methoxy group at the C-5 position, resulting in a higher proportion of 5–5 and 4–O–5 linkages than in hardwoods containing S units. These linkages exhibit relatively low reactivity under catalytic hydrogenolysis. Overall, Japanese beech (hardwood) is more favorable for producing aromatic monomers than Japanese cedar (softwood), particularly at lower temperatures. At higher temperatures (400 °C), the difference diminishes, and such conditions are effective for achieving high yields from softwood. As noted above, softwood lignin composed solely of G units produces simpler monomer compositions than hardwood lignin containing S units, but at 400 °C these compositional differences disappear as the S and G units gradually transition to catechols and phenols (Fig. S6).

When the temperature was increased to 450 °C, the aromatic monomer yield after 60 min decreased, particularly for Japanese beech (from 68.9 mol% at 400 °C to 23.1 mol% at 450 °C/60 min). In Japanese beech, catechol units disappeared and were replaced entirely by phenol units. However, after only 5 min at 450 °C, the aromatic monomer yields remained relatively high—55.9 mol% for Japanese beech and 57.7 mol% for Japanese cedar—and the conversion to phenol and catechol units was nearly complete, resulting in a similar monomer composition for both species (Fig. S7).

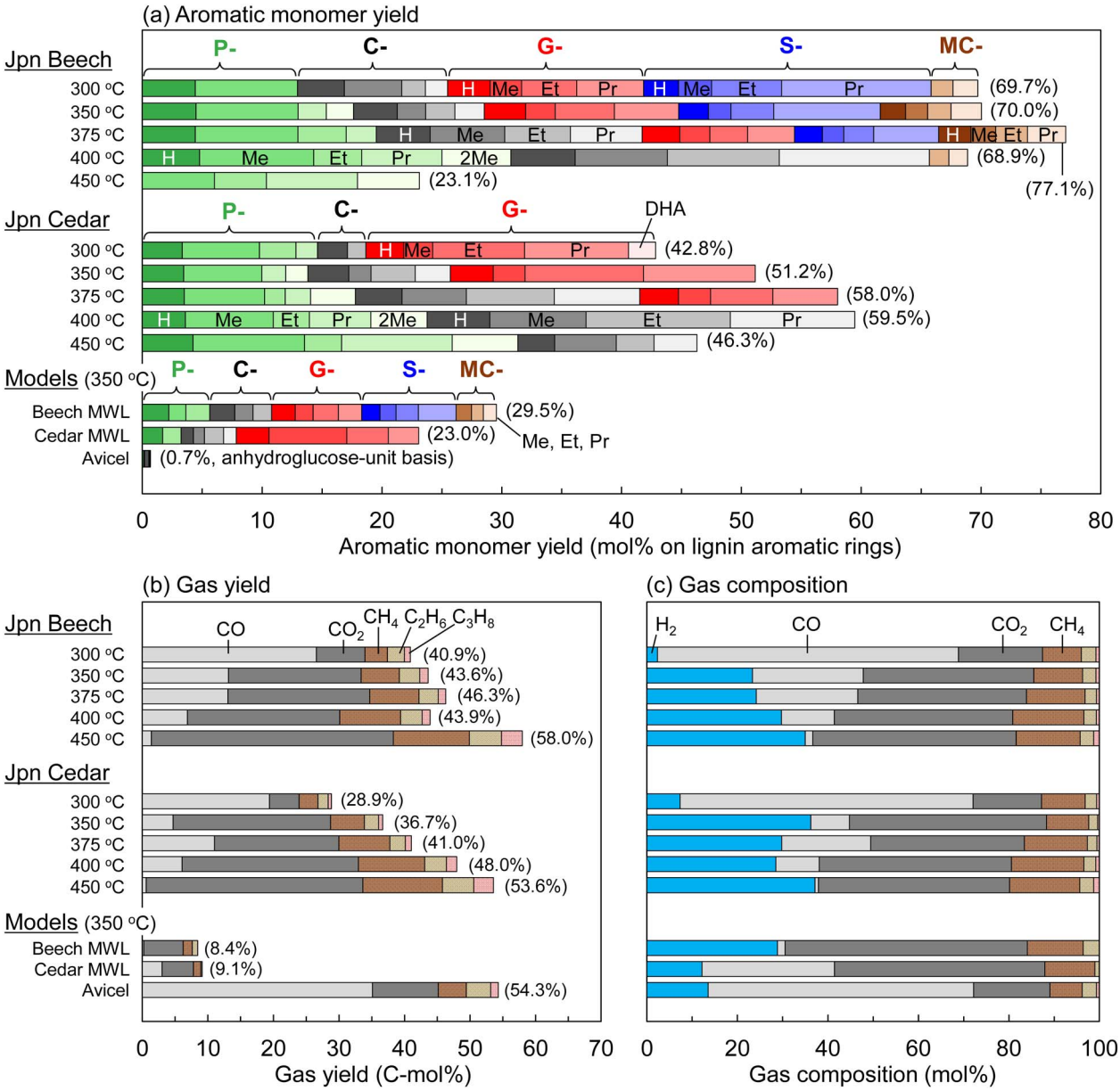

Fig. 2 Yields of (a) aromatic monomers, (b) gaseous products, and (c) gas composition from Japanese beech and Japanese cedar (100 mg) and from isolated lignin and cellulose samples (25–100 mg), treated at various temperatures for 60 min in H_2O (1 mL) under N_2 over Pd/C (25 mg). Values in parentheses indicate the total yield of aromatic monomers or gases. Gas yields are expressed as *C*-mol% on a polysaccharide basis for wood and Avicel, and on a phenylpropanoids basis for MWL.

Regarding gaseous products, increasing the temperature from 400 °C to 450 °C led to a rise in gas yields from 43.9 mol% to 58.0 mol% for Japanese beech and from 48.0 mol% to 53.6 mol% for Japanese cedar after 60 min (Fig. 2). At 450 °C/5 min, both woods produced nearly 60 mol% gas, with a substantial proportion of methane, and increased fractions of ethane and propane compared to lower temperature treatments (Fig. S7). These findings suggest that a portion of the lignin-derived aromatic monomers was gasified.

Supporting this, the ^{1}H NMR spectrum of the fraction directly extracted with $CDCl_3$ from the 450 °C product of Japanese beech revealed strong signals in the hydrocarbon region, including that of cyclohexane, indicating partial hydrogenation of benzene rings and subsequent gasification *via* cyclohexane derivatives (Fig. S8). Consistently, the gas composition at 450 °C showed increased formation of methane, ethane, and propane from both Japanese beech and Japanese cedar, supporting the interpretation that these gases originated through cyclohexane intermediates.

For the model compounds, the aromatic monomer compositions obtained from MWL of Japanese beech and Japanese cedar were similar to those from whole wood, but the yields were lower (29.5 mol% and 23.0 mol%, respectively) at 350 °C. In contrast, higher yields were obtained from wood containing

polysaccharides. It has been reported that the hydroxypropyl side chains of lignin can act as hydrogen donors, and the resulting hydrogen promotes catalytic hydrogenolysis in MWL conversion as well.[24] However, the amount of hydrogen generated during wood treatment is far greater, indicating that catalytic hydrogenolysis of lignin pyrolysis products proceeds more efficiently in wood than in MWL.

A small amount of aromatic monomers (0.7 mol% on a glucose-unit basis), including catechol, methylcatechol, ethylcatechol, phenol, and methylphenol, was also produced from Avicel. These are likely attributable to trace amounts of residual lignin in Avicel.

Syngas production

Comparison of Avicel and MWL showed that gas yields were much higher for Avicel (Fig. 2), confirming that gases originated mainly from polysaccharides in wood (gas yields from MWL are given on a carbon basis). The main product was CO, accompanied by H_2, CO_2, and small amounts of methane and ethane. For Japanese beech and Japanese cedar in the 300–400 °C range, beech gave nearly constant gas yields excluding hydrogen (40.9–46.3 mol% on a polysaccharide carbon basis), whereas cedar showed an increase from 28.9 mol% to 48.0 mol% with rising temperature. This trend mirrors that observed for aromatic monomers. These results suggest that both lignin and polysaccharides exhibit higher pyrolytic reactivity in Japanese beech than in Japanese cedar. Our previous work with five softwood and five hardwood species[25,26] demonstrated that hardwood hemicelluloses are more reactive than those of softwoods. At 450 °C, gas yields increased to 58.0 mol% for beech and 53.6 mol% for cedar, likely due to decomposition of aromatic monomers, as discussed above.

Regarding gas composition, CO was the main component at 300 °C, accompanied by CO_2 and small amounts of H_2 and CH_4. With increasing temperature, CO decreased while CO_2 and H_2 increased. At 450 °C/60 min, CO was almost completely consumed, and the gases consisted mainly of H_2 and CO_2 (Fig. 2). This change can be explained by the progress of the water-gas shift (WGS) reaction ($CO + H_2O \rightarrow H_2 + CO_2$). The generated H_2 is utilized in the hydrogenolysis of lignin-derived products. In the 350–450 °C range, the extent of WGS progression depended more on the treatment duration rather than on the temperature (Fig. 2 and S5–S7). In contrast, as discussed above, the treatment temperature played a more significant role in determining the composition of aromatic monomers. Accordingly, gas composition can be adjusted independently of aromatic monomer composition by selecting an appropriate combination of temperature and duration.

Methane was also produced from Avicel; however, as discussed later, part of the methane formed from wood may originate from methyl radicals generated through demethylation of methoxy groups on the aromatic rings.

Lignin conversion mechanisms

GPC analyses of the EtOAc-soluble fractions (mainly lignin-derived products) obtained from Japanese beech and Japanese cedar under different treatment temperatures and times are shown in Fig. 3. In addition to the conditions in Fig. 1 and 2, a short-time treatment (5 min) at 300 °C was also examined. At 300 °C, signals were observed in the high-molecular-weight region near the upper detection limit (1500 Da), and with increasing temperature the signals shifted toward longer elution times (lower molecular weight). These results suggest that thermal degradation of the wood cell wall first solubilizes high-molecular-weight lignin-derived products, which are then depolymerized into lower-molecular-weight compounds through catalytic hydrogenolysis.

HSQC NMR spectra of the EtOAc-soluble fractions from Japanese beech obtained under conditions of 300 °C/5 min, 300 °C/60 min, and 350 °C/60 min are compared in Fig. 4. The identified structures are depicted in Chart 1. The aromatic monomers shown in Fig. 2 were identified by GC-MS, and therefore no information was obtained for oligomeric or polymeric products. The NMR spectra, however, enables a discussion of the chemical structures present in the higher-molecular-weight region.

Even under the 300 °C/5 min condition (aromatic monomer yield: 23.1 mol%), signals corresponding to the β-ether structures—the most abundant linkages in lignin—had nearly disappeared in the δ_C/δ_H 40–90/2.5–5.5 ppm region. This suggests that in lignin-derived oligomers and polymers, monomer units are connected not by ether linkages between side chains and

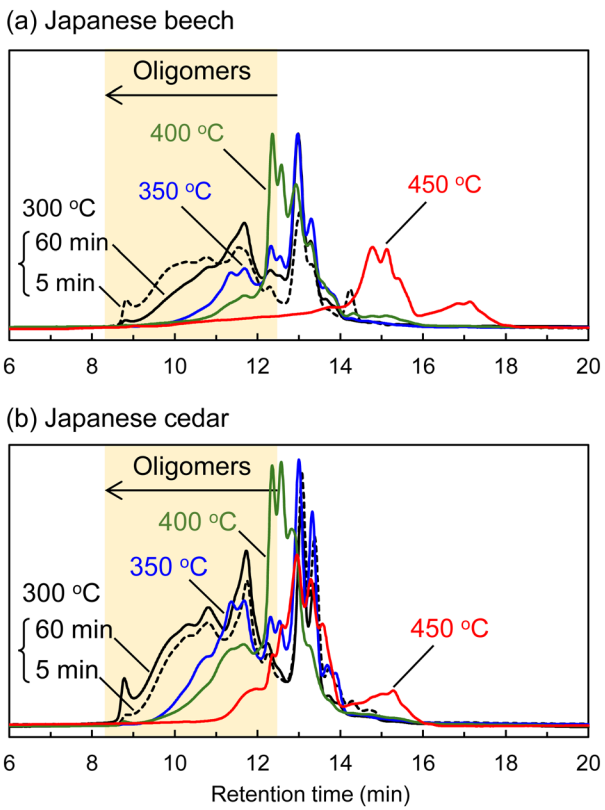

Fig. 3 Gel permeation chromatograms of EtOAc-soluble products from (a) Japanese beech and (b) Japanese cedar (100 mg), treated in H_2O (1 mL) under N_2 over Pd/C (25 mg).

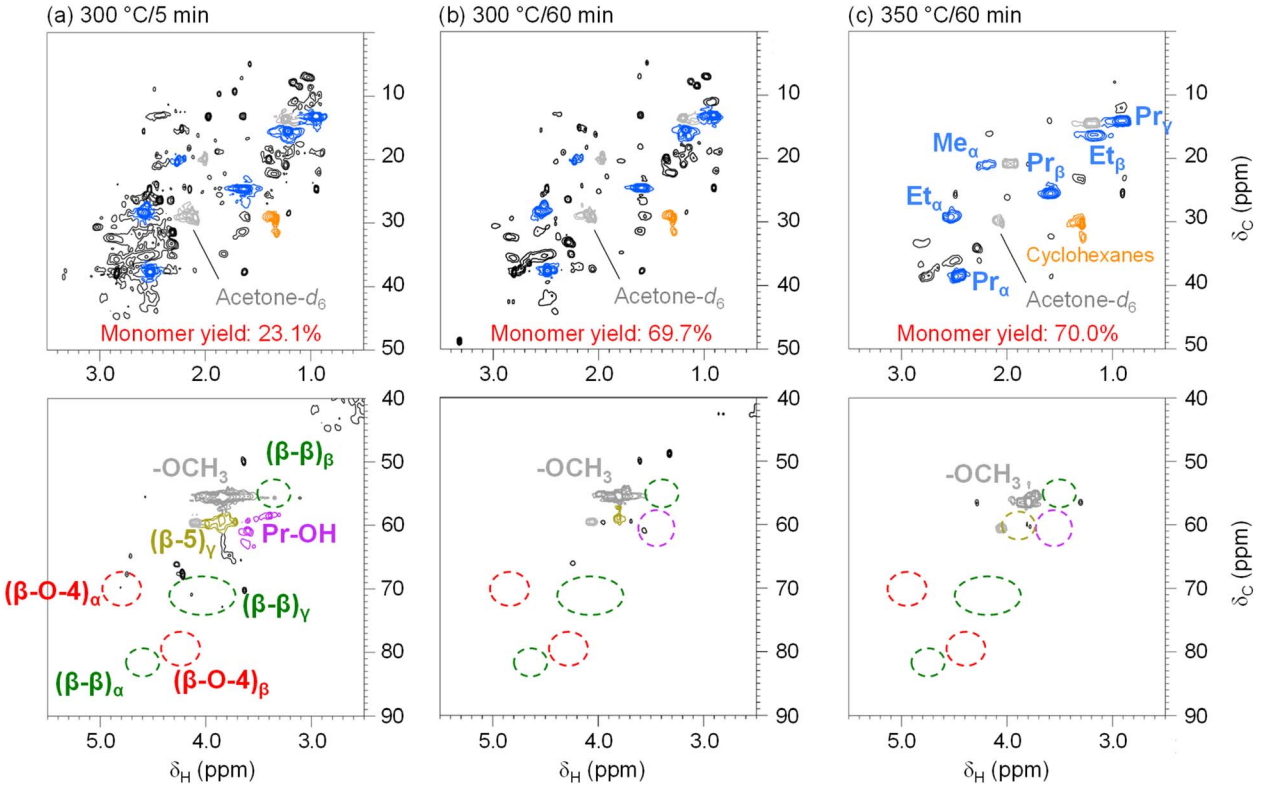

Fig. 4 HSQC-NMR spectra (400 MHz, acetone-d_6) of EtOAc-soluble products obtained from Japanese beech wood (100 mg) at (a) 300 °C/5 min, (b) 300 °C/60 min and (c) 350 °C/60 min over Pd/C in H2O (1 mL) under N_2 atmosphere (1 atm, prior to heating). Signals from unidentified structures shown in black.

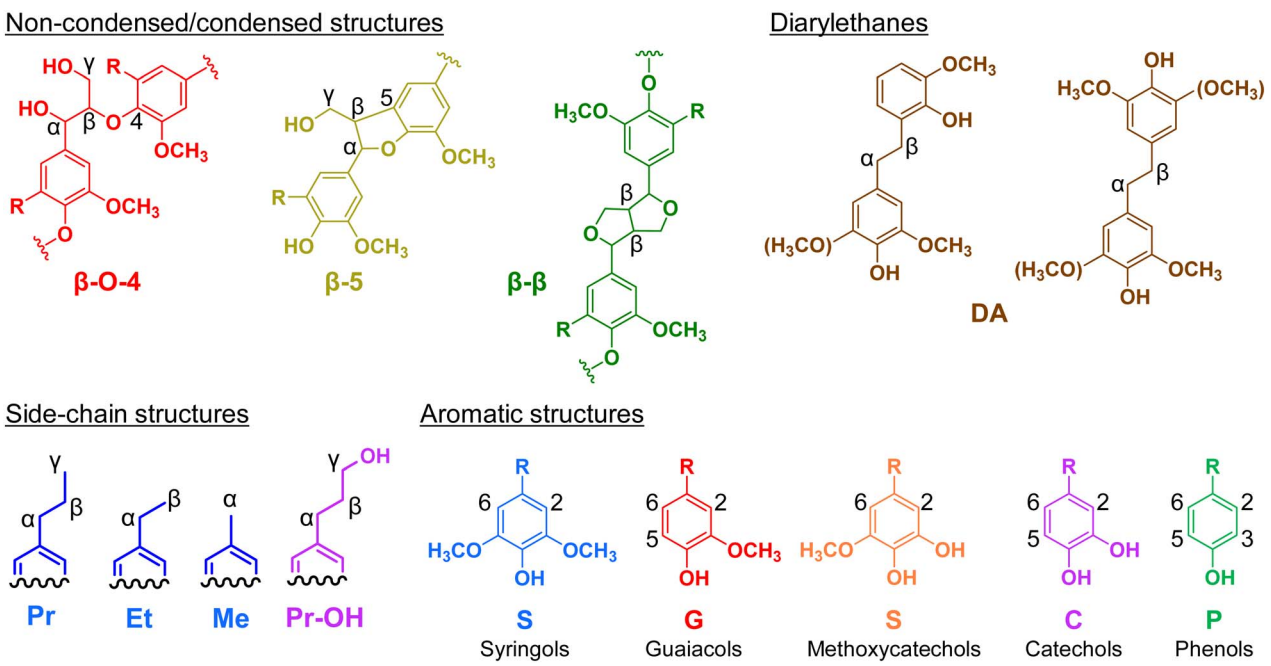

Chart 1 Chemical structures identified by HSQC-NMR spectroscopy (400 MHz).

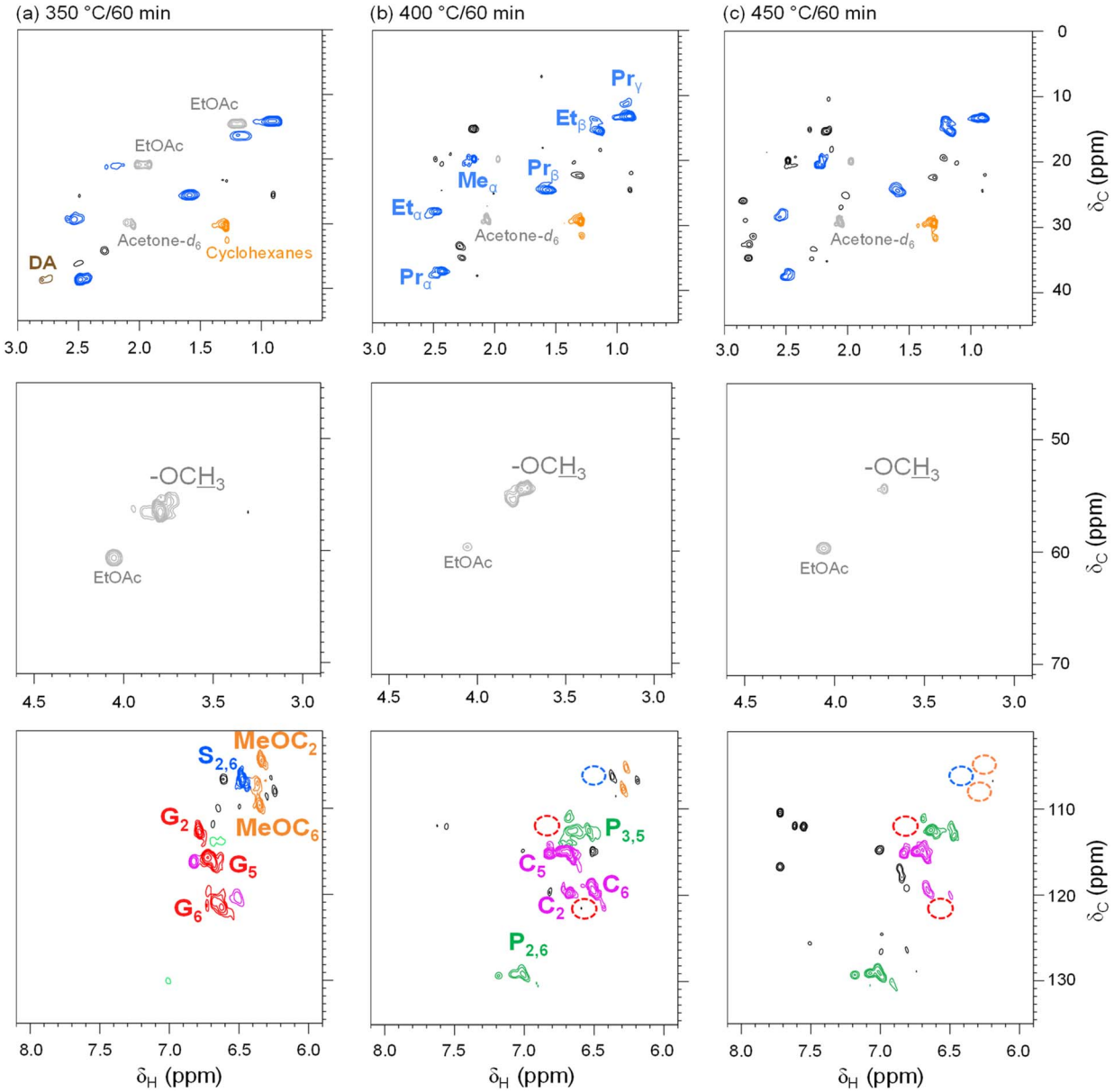

Fig. 5 HSQC-NMR spectra (400 MHz, acetone-d_6) of EtOAc-soluble products obtained from Japanese beech wood (100 mg) at (a) 350 °C/60 min, (b) 400 °C/60 min and (c) 450 °C/60 min over Pd/C in H2O (1 mL) under N_2 atmosphere (1 atm, prior to heating). Signals from unidentified structures shown in black.

aromatic rings but rather through C–C and diphenyl ether bonds. This interpretation is further supported by the presence of broad signals in the hydrocarbon region (δ_C/δ_H 0–50/0.5–3.5 ppm).

The cell wall is a nanoscale composite in which cellulose microfibrils are surrounded by a hemicellulose–lignin matrix, preventing access of the solid Pd/C catalyst. Our previous work using aromatic solvents showed that lignin-derived aromatic monomers dissolve into the medium when cellulose, which is more thermally stable than lignin, begins to decompose actively.[11,27] This indicates that lignin β-ether bonds are cleaved mainly by thermal degradation, and the resulting fragments undergo catalytic conversion after dissolution. Even when β-ethers remain in solubilized oligomers, they are likely cleaved readily by the catalyst.

Extending the treatment time at 300 °C from 5 to 60 min simplified the signals in the hydrocarbon region, and under the 350 °C/60 min condition, signals from methyl, ethyl, and propyl groups—side chains of aromatic monomers—became dominant. These results suggest that thermally stable linkages, such as C_α–aryl structures formed by condensation and diphenyl ether (4–O–5) structures, are cleaved under more severe conditions.[20] Correspondingly, aromatic monomer yields increased

from 23.1 mol% (300 °C/5 min) to 69.7 mol% (300 °C/60 min) and 70.0 mol% (350 °C/60 min).

In the 350–450 °C range, the substitution patterns of the aromatic nuclei in the monomers changed drastically from G and S units to catechol and then to phenol units. This transformation is discussed for higher-molecular-weight products using the HSQC NMR spectra of Japanese beech (Fig. 5). In the aromatic region of Fig. 5a (δ_C/δ_H 100–135/6–8 ppm), signals from G and S units were dominant at 350 °C, whereas at 400 and 450 °C they shifted to catechol and phenol units. This indicates that the same transformations observed for monomers also occur in higher-molecular-weight lignin-derived products. At 450 °C, catechol signals were still present, suggesting that the conversion from catechol to phenol occurs more rapidly in monomers. This trend is further supported by the weakening of methoxy signals with increasing temperature in Fig. 5b. At 450 °C, unidentified black signals appeared in the aromatic region, implying the presence of aromatic nuclei and substituents distinct from those formed at lower temperatures, although their detailed structures remain unclear.

In the hydrocarbon region (δ_C/δ_H 0–50/0.5–3.5 ppm, Fig. 5c), strong signals from methyl, ethyl, and propyl groups were observed under all temperature conditions, similar to those in the monomers. At 350 °C, signals from diarylethane (formed from phenylcoumaran structures *via* stilbene) were detected, suggesting its relatively low reactivity toward cleavage. These signals disappeared at ≥400 °C, indicating decomposition. In fact, diarylethane-type dimers with various substituents, along with 5–5 (biphenyl) type dimers, were detected in the GC-MS analysis of the EtOAc-soluble fractions (Fig. S9–S12). These dimer signals were particularly prominent in Japanese cedar and decreased in intensity with increasing treatment duration at 350 °C, which correlated with increasing aromatic monomer yields.

In all spectra, a peak near δ_C/δ_H 30/1.3 ppm was assigned to cyclohexane rings generated by hydrogenation of benzene rings. The absence of signals in the δ_C/δ_H 40–90/3–4.5 ppm region suggests that the cyclohexane rings lacked ether or hydroxyl substituents. These results imply that cyclohexane rings were also formed in the monomer region detectable by GC-MS, but they were likely lost during vacuum concentration of the EtOAc fraction. Consistently, the ^{1}H NMR spectrum of the fraction directly extracted with $CDCl_3$ from the 450 °C product of Japanese beech showed a sharp signal near δ_H 1.3 ppm, attributable to cyclohexane (Fig. S8). Nevertheless, because aromatic monomer yields remained high below 400 °C (Fig. 2), hydrogenation of benzene rings is not considered significant under these milder conditions.

In the spectra at 400 and 450 °C, new unidentified signals appeared in the δ_C/δ_H 10–40/2–3 ppm region, suggesting the formation of new hydrocarbon structures. These products are likely generated through hydrogenation of aromatic rings and contribute to the decrease in aromatic monomer yields.

Based on these results and previous studies, the proposed conversion mechanisms are summarized in Fig. 6 and 7. Fig. 6 illustrates the transformations involving linkages between the benzene ring and the propyl side chain in lignin, while Fig. 7 shows the transformations of methoxy groups. The α- and β-ether bonds in lignin are readily cleaved during pyrolysis to selectively yield cinnamyl alcohols such as sinapyl alcohol and coniferyl alcohol.[28,29] These hydroxyprop-2-enyl groups (–CH = CH–CH_2OH) are further decomposed into propenyl (–CH = CH–CH_3), vinyl (–CH = CH_2), and conjugated aldehyde (–CH = CH–CHO) groups.[30] Products bearing such conjugated C=C structures are easily transformed into quinone methides, which subsequently condense with benzene rings at the α and γ positions to form recondensation products.[31] In this process, new thermally stable C–C bonds are generated. On the other hand, β-aryl, biphenyl, and diphenyl ether structures are resistant to pyrolytic cleavage, and oligomers containing these linkages are therefore formed.[20]

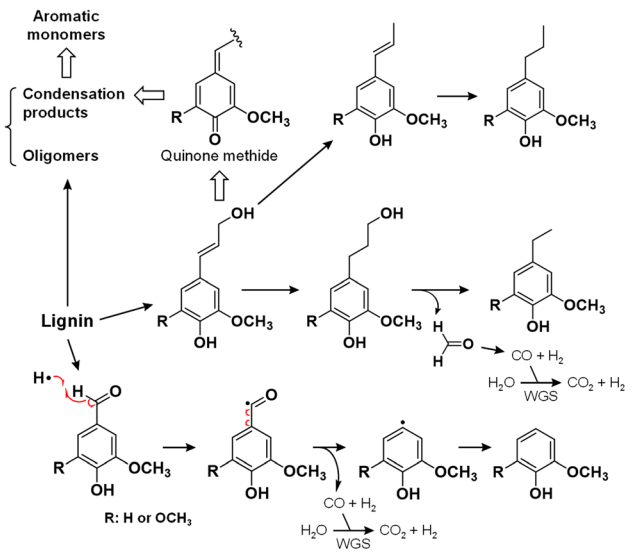

Fig. 6 Proposed conversion mechanisms of lignin in wood to aromatic monomers *via* pyrolysis followed by catalytic hydrogenolysis.

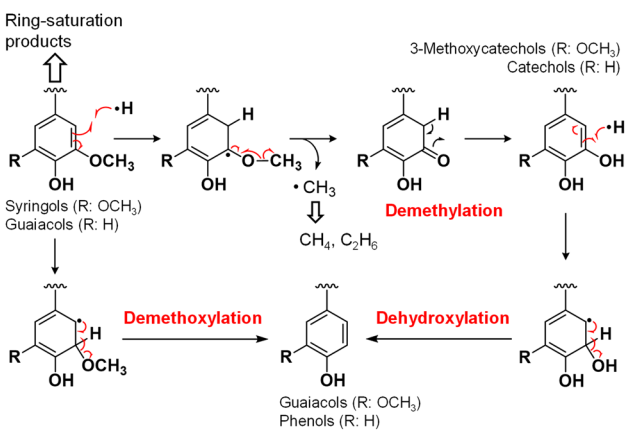

Fig. 7 Proposed mechanisms of methoxyl group demethylation, demethoxylation and dehydroxylation of aromatic rings from lignin-derived products.

These pyrolysis products are further converted over the Pd/C catalyst. Hydrogenation of C=C structures stabilizes them against quinone methide formation, thereby suppressing recondensation and converting the side chains into ethyl and propyl groups. In addition, hydroxypropyl groups are transformed into ethyl groups through deformylation.[24] Intermediates such as dihydrosinapyl alcohol and dihydro coniferyl alcohol are involved in this process, and these products are observed under milder conditions.

In parallel, cleavage of the C_α–C_β bond in lignin side chains proceeds during pyrolysis, producing syringaldehyde and vanillin.[29] These compounds undergo deformylation to yield syringol and guaiacol, with part of the products further converted into methyl groups.[24] The formaldehyde generated by deformylation is subsequently transformed into CO and H_2, and CO is further converted into H_2 and CO_2 *via* the WGS reaction. The H_2 thus formed is utilized in the catalytic hydrogenolysis of lignin-derived products. As these reactions proceed, one carbon atom from each lignin repeating unit (C_{11} for S units and C_{10} for G units) is converted into gas. If this occurs for all units, the theoretical gas yields on a carbon basis would be 9.1% and 10%, respectively, which rationally explain the observed gas yields of 8.4% and 9.1% from MWL of Japanese beech and Japanese cedar (Fig. 2). In practice, additional gas formation is also expected from reactions of methoxy groups.

As described above, the structures of the aromatic monomers change with increasing treatment temperature, following the sequence S and G → catechol → phenol units. This can be explained by a mechanism in which hydrogen activated on the catalyst (as hydrogen radicals) adds to the benzene ring, forming a non-aromatic radical intermediate (Fig. 7). Upon re-aromatization, β-scission reaction occurs. When ˙H adds to carbons ortho or para to a methoxy group, the carbon bonded to the methoxy group becomes a radical center. Subsequent β-scission of the methoxy methyl group produces a ketone, which rearranges to a phenol structure, thereby promoting demethylation of the methoxy group and leading to the formation of catechols. During this process, methyl radicals are generated as precursors of gaseous methane and ethane. Indeed, methane and ethane production increased in parallel with rising catechol levels (Fig. 2 and S6). Similarly, addition of ˙H to carbons bearing methoxy or hydroxyl substituents induces demethoxylation and dehydroxylation. Hydrolysis of the methoxy group is also possible under hot-compressed water, but this reaction did not proceed without Pd/C, supporting the homolytic mechanism.

Gas formation mechanisms from wood polysaccharides

The water-soluble fractions obtained from Japanese beech and Avicel under the 350 °C/60 min condition were analyzed by GC-MS after evaporation and subsequent trimethylsilylation, and the results are shown in Fig. 8. Ethylene glycol, lactic acid, glycolic acid, levulinic acid, glycerol, and succinic acid were identified, indicating the presence of C_2–C_4 polyalcohols and organic acids. The amount of the water-soluble fraction was relatively small, while a large quantity of gas was generated (Fig. 1), suggesting that the compounds identified in this fraction are by-products with relatively low reactivity toward gasification.

Among these products, lactic acid, levulinic acid, and succinic acid are important biochemicals derived from sugars, and the formation mechanisms of lactic acid and levulinic acid have been extensively studied. Lactic acid is known to form when glucose is isomerized to fructose, followed by a retro-aldol reaction producing glyceraldehyde, which undergoes dehydration *via* a six-membered transition state (Fig. 9).[32,33] Levulinic acid is considered to form from fructose through the intermediate 5-hydroxymethyl furfural, generated by cyclization and dehydration reactions.[34,35] These findings indicate that retro-aldol and dehydration reactions of sugars are occurring. Moreover, because the treatment was conducted in hot-compressed water, it is reasonable to assume that cellulose and hemicellulose hydrolysis is also likely to have contributed to sugar formation.[36–38]

From these considerations, the pathway on the right side of Fig. 9 is proposed as the gasification mechanism. Glucose undergoes a retro-aldol (RA) reaction to form glycolaldehyde (GA) and a C_4 sugar. Then, two different pathways are proposed. First, the C_4 fragment is further converted into two GA molecules through another RA step. Alternatively, the aldehydic hydrogen on this C_4 sugar is then abstracted by ˙H to form H_2 and a C_4 fragment containing a formyl radical end. This formyl radical end undergoes α-scission, producing CO and a C_3 radical. The C_3 radical then undergoes β-scission to regenerate a C_3 sugar. Thus, this reaction continuously

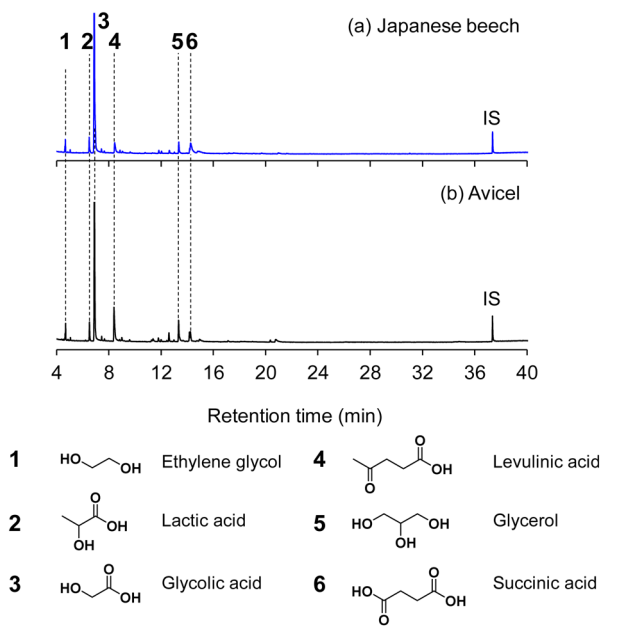

Fig. 8 GC/MS total-ion chromatograms of H_2O-soluble products after trimethylsilylation obtained from (a) Japanese beech wood (100 mg) and (b) Avicel cellulose (100 mg) in H_2O (1 mL) under N_2 atmosphere (1 mL, prior to heating) over Pd/C (25 mg) at 350 °C for 60 min. Internal standard (IS): 1,3,5-triphenylbenzene.

generates CO and H_2 while successively regenerating sugars shortened by one carbon atom. GA is similarly transformed into CO and H_2, and the same sequence of reactions can also occur directly from glucose. The formation of ethylene glycol and glycolic acid can also be explained by hydrogenation of GA and by the reaction of formyl radicals derived from GA with OH radicals.

Influence of polysaccharide components

To further examine the influence of polysaccharides, guaiacol, syringol, and methylsyringol were used as model compounds of lignin-derived products. Their reactivity was studied under a hydrogen atmosphere at 350 °C for 60 min in the presence of Avicel or glycerol (a model of water-soluble products derived from polysaccharides). The results are shown in Fig. 10. In addition, experiments were conducted in hexane rather than water under two gas atmospheres, H_2/N_2 (1 : 1, v/v) and H_2/CO (1 : 1, v/v), to investigate the effect of CO derived from polysaccharides on the catalytic hydrogenolysis of lignin-derived products. Hexane was used instead of water because in aqueous media CO is converted to CO_2 and H_2 *via* the WGS reaction, and this conversion was to be suppressed. Furthermore, to detect low-boiling products that might otherwise volatilize and be lost during concentration of the EtOAc-soluble fraction, the reaction mixtures were directly extracted with $CDCl_3$, and the lignin-derived products from the model compounds were quantified by ^1H NMR spectroscopy.

Under a hydrogen atmosphere, guaiacol was converted sequentially *via* guaiacol → catechol → phenol → benzene, giving benzene (43.6 mol%, at 73.5% selectivity) and phenol (14.0 mol%, at 23.6% selectivity) as the major products. When glycerol was added, the reaction rate was greatly reduced, and 52.0% of guaiacol was recovered, with only small amounts of catechol (7.9 mol%) and phenol (3.6 mol%) produced. These results suggest that glycerol, present in the water-soluble fraction, inhibits the catalytic reaction. A similar trend was observed for syringol, and the conversion pathway was suggested to proceed *via* syringol → methoxycatechol → guaiacol → catechol → phenol → benzene. In the case of methylsyringol, catalytic conversion was also suppressed when Avicel was added. In contrast, when CO was added to the hydrogen atmosphere, the catalytic conversion of syringol was hardly affected.

From these results, the roles of wood polysaccharides, as illustrated in Fig. 11, were clarified. As described above, lignin and wood polysaccharides decompose within the cell wall by pyrolysis until cellulose begins to decompose extensively. Upon solubilization in hot-compressed water, these products become accessible to the catalyst and are further converted by catalytic hydrogenolysis. In this process, water-soluble polysaccharide-derived products mainly inhibit

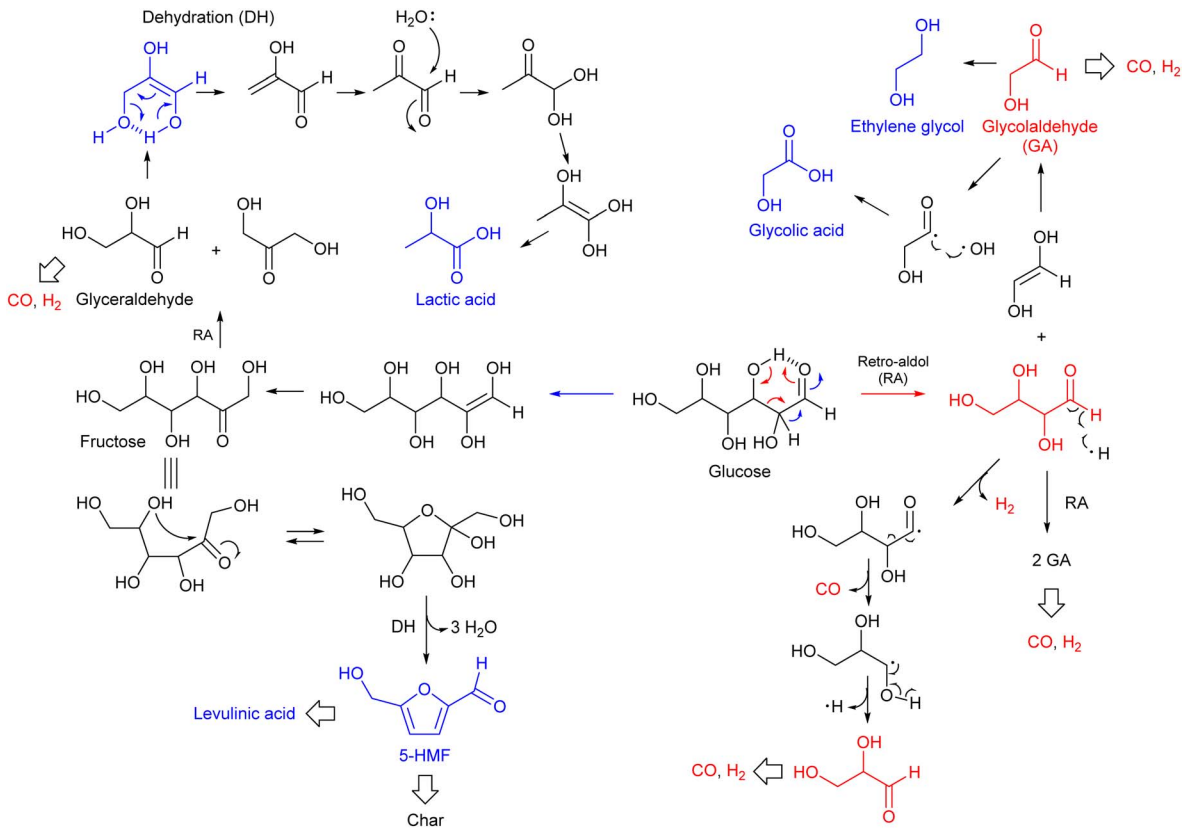

Fig. 9 Proposed conversion pathways of wood polysaccharides to syngas and water-soluble products.

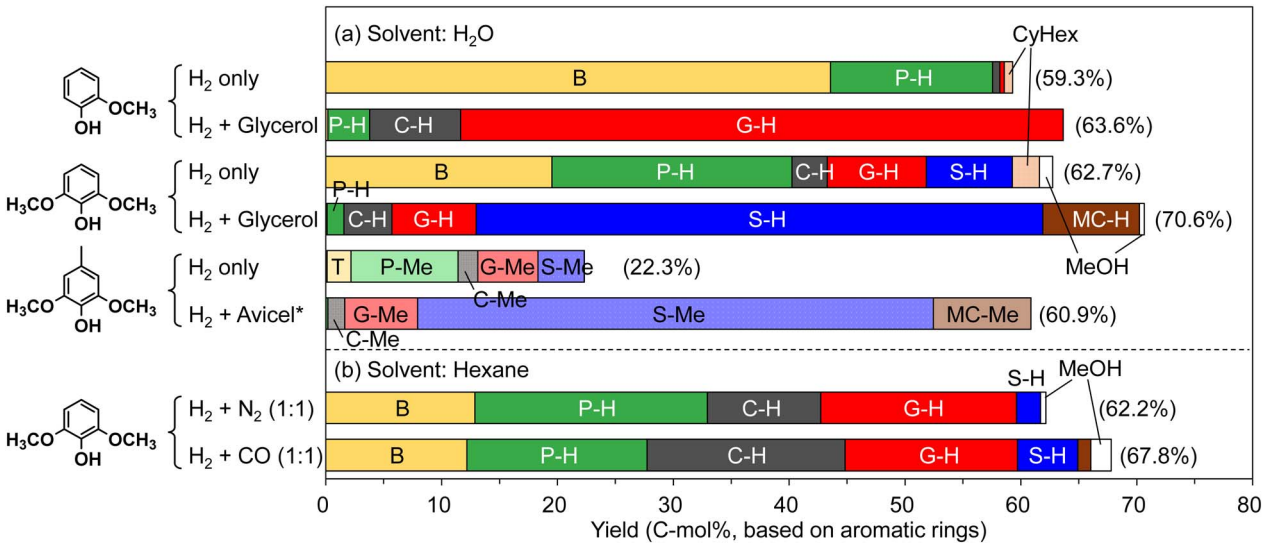

Fig. 10 Effects of adding glycerol, Avicel cellulose and carbon monoxide (CO) on the yields of monomeric products obtained from guaiacol, syringol and methyl syringol as aromatic model compounds at 350 °C for 60 min in (a) H_2O or (b) hexane (1 mL) under H_2 atmosphere (1 atm, prior to heating) over Pd/C. MeOH: methanol, CyHex: cyclohexane, B: benzene, T: toluene, P: phenol, C: catechol, G: guaiacol, S: syringol, MeOC: methoxycatechol, MP: methyl phenol, MC: methyl catechol, MG: methyl guaiacol, MS: methyl syringol, MeOMC: methyl methoxycatechol. *The yield of aromatic monomers from Avicel was negligible.

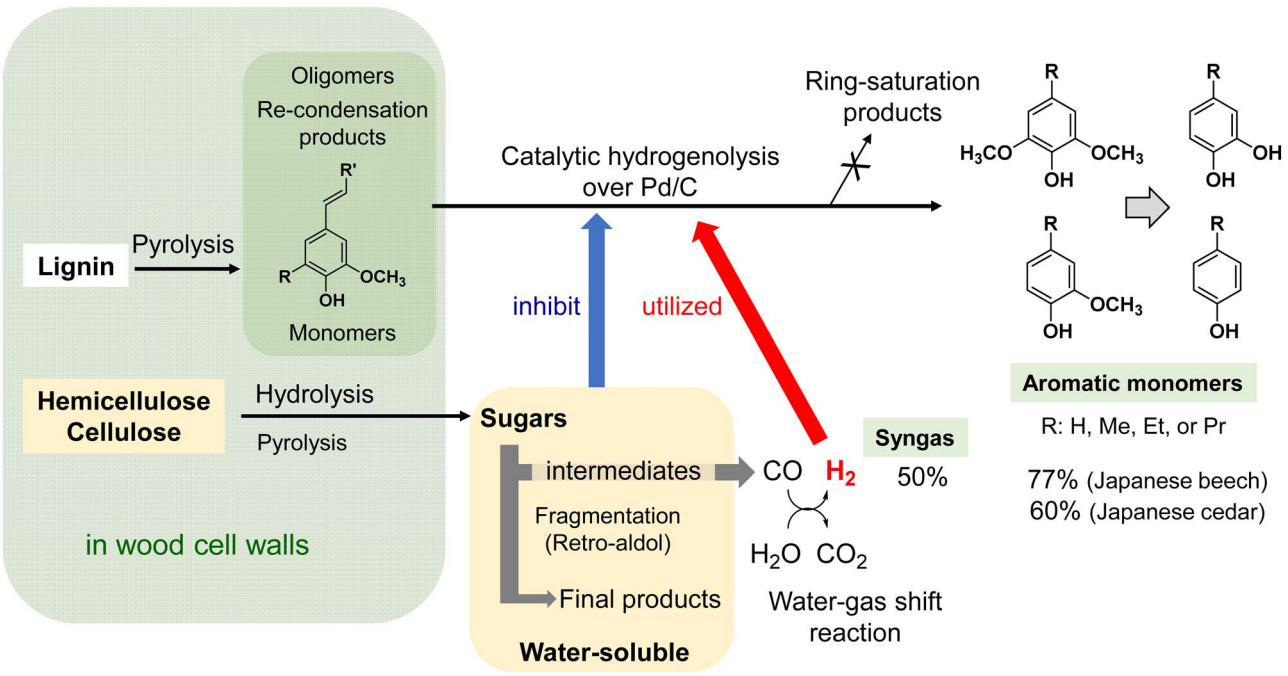

Fig. 11 Roles of wood polysaccharide-derived products on pyrolysis-assisted catalytic hydrogenolysis of wood lignin in hot-compressed water.

catalytic activity through competitive adsorption, but this inhibitory effect is mitigated as they are gasified. The hydrogen produced plays a promoting role in catalytic hydrogenolysis, ultimately leading to high yields of both syngas—usable for methane or Fischer–Tropsch synthesis—and aromatic monomers. Thus, wood polysaccharides act as modulators of catalytic hydrogenolysis, and the present reaction conditions were found to provide reactivity conditions that are well suited for the production of syngas and aromatic monomers.

The results obtained here provide crucial insights for the production of biochemicals and biofuels from lignocellulosic biomass such as wood and herbaceous plants.

Conclusions

1. Treatment of Japanese cedar or Japanese beech in hot-compressed water at temperatures above 300 °C over Pd/C produces aromatic monomers and syngas in high yields without external hydrogen. The monomer composition shifts from guaiacols and syringols at lower temperatures to catechols and phenols above 400 °C, regardless of wood species.

2. Wood polysaccharides are hydrolyzed to monosaccharides, which undergo fragmentation to yield syngas. CO is subsequently converted to CO_2 and H_2 *via* the water-gas shift (WGS) reaction, enabling polysaccharides to serve as an *in situ* hydrogen source for lignin hydrogenolysis and suppressing lignin re-polymerization.

3. Polysaccharide-derived products are solubilized in hot-compressed water and can inhibit catalyst activity through competitive adsorption. However, this inhibition diminishes as these intermediates are gasified, allowing sustained and efficient conversion. These findings provide insights for developing biomass-based alternatives to petroleum-derived chemical processes.

Experimental

Materials

Extractive-free Japanese cedar (*Cryptomeria japonica*, a softwood) and Japanese beech (*Fagus crenata*, a hardwood) of particle size below 150 μm were prepared in accordance with our previous work.[39] Milled wood lignins (MWLs) from both wood species were isolated using the methods described by Bjorkman.[40] Microcrystalline cellulose (Avicel PH-101, particle size: 50 μm, Sigma-Aldrich, United States) was used as a model for cellulose *in planta* without prior modification. The water content of the wood samples and Avicel ranged from 7 to 8 wt%. 5% Pd/C (extra-pure grade, Nacalai Tesque Inc., Kyoto, Japan) was used as a heterogeneous catalyst. The as-purchased Pd/C catalyst was subjected to X-ray diffraction analysis (XRD) using a Rigaku RINT 2000V diffractometer (Rigaku, Tokyo, Japan). The obtained XRD pattern (Fig. S22) was consistent with those reported elsewhere.[41] Deionized water was prepared using a Milli-Q integral 3 (Merck Millipore, Burlington, United States) ultrapurification system and hexane (guaranteed reagent grade, Nacalai Tesque Inc., Kyoto, Japan) were used as solvent media for pyrolysis. Guaiacol (2-methoxyphenol, Nacalai Tesque Inc., Kyoto, Japan), syringol (2,6-dimethoxyphenol, Wako Pure Chemical Industries, Osaka, Japan), methyl syringol (2,6-dimethoxy-4-methylphenol, Tokyo Kasei Kogyo Inc., Tokyo, Japan), glycerol (guaranteed reagent grade, Nacalai Tesque Inc., Kyoto, Japan) were used as purchased without further modification. Ethyl acetate (guaranteed reagent grade, Nacalai Tesque Inc., Kyoto, Japan) was used as an organic solvent in the product fractionation steps.

Catalytic pyrolysis in hot-compressed water with a batch reactor

Fixed amounts of ground wood (100 mg), Pd/C catalyst (25 mg) and deionized water (1.0 mL, 25 °C) were added to the bottom of an Inconel 625 batch reactor (Fig. S1). The loaded vessel (internal volume: 5 mL) was then inserted into a plastic bag connected to a water aspirator system and the atmosphere inside the reaction chamber was replaced with N_2 (0.1 MPa). After this, the reactor was sealed and immersed in a preheated salt bath at 300–450 °C for 5–60 min. Upon immersion, the time required for reaching the target temperature was approximately 40 s. After the designated reaction time, the reactor was immediately quenched in a water bath at room temperature for 3 min. Experiments with model compounds were performed at 350 °C/60 min using Japanese beech MWL (25 mg), Japanese cedar MWL (33 mg) and microcrystalline cellulose (100 mg) as starting materials instead of ground wood. Experimental runs with monomers as starting materials were done at a smaller scale under either a N_2 or H_2 atmosphere (1 atm) at 350 °C/60 min, using 20 mg of starting material, 20 mg of Pd/C catalyst and an optional addition of 20 mg of microcrystalline cellulose (Avicel) or glycerol.

Product fractionation and analysis

A schematic diagram of the fractionation methods used in this study is shown in Fig. S2. After pyrolysis, the reactor was inserted into a polypropylene gas bag, which was sealed and degassed with a water aspirator. Then, the reactor was carefully opened inside the sealed gas bag to allow for the collection of non-condensable gaseous products. The gaseous products were analyzed and quantified by Micro GC (Agilent 990, Agilent Technologies Inc., Santa Clara, CA, USA) following a procedure described by Minami *et al.*[42] The reactor contents were washed alternately with ethyl acetate (EtOAc) and distilled water, resulting in a slurry containing the spent Pd/C catalyst and approximately 25 mL of a 1 : 1 (v/v) biphasic mixture. This mixture was subjected to vacuum filtration. The collected aqueous and EtOAc-fractions were then transferred to a 50 mL separatory funnel, mixed, and allowed to separate. The EtOAc-soluble fraction, which contained the lignin-derived products, was collected first and subjected to chemical drying over anhydrous sodium sulfate (Na_2SO_4, Nacalai Tesque Inc., Kyoto, Japan). Both fractions were then concentrated *via* vacuum evaporation. The solid residue fraction, which contained the spent catalyst and wood-derived char was oven-dried at 100 °C for 2 h prior to gravimetric analysis using an analytical balance.

The char yield was determined as follows:

$$\text{Char yield (wt\%)} = \frac{\text{mass of solid residue} - \text{mass of catalyst}}{\text{mass of wood sample}} \times 100\%$$

For the experiments using guaiacol, syringol and 4-methyl syringol as starting materials, the reactor contents were immediately washed with 3 mL chloroform-d ($CDCl_3$, δ_H: 7.26 ppm) and approximately 10 mL of distilled water after gas analysis, resulting in a slurry containing Pd/C, $CDCl_3$ and water. This slurry was centrifuged using a MF12000 microcentrifuge (AS ONE Co., Osaka, Japan) at 10^4 rpm for 20 s to separate the spent Pd/C catalyst. The aqueous and $CDCl_3$-soluble fractions

were then recollected, combined in a separatory funnel, mixed and allowed to separate. The $CDCl_3$-soluble fraction was isolated and dried over Na_2SO_4. Subsequently, 0.7 mL of the $CDCl_3$ fraction was mixed with dimethyl sulfone (purity: 99.0%, δ_H: 2.98 ppm, Tokyo Kasei Kogyo Inc., Tokyo, Japan) as an internal standard for ^1H NMR analysis, which was performed on a Bruker AC-400 spectrometer (400 MHz, Varian Medical Systems, Palo Alto, CA, USA). Acetone-d_6 (δ_H: 2.05 ppm) was used as the deuterated solvent for HSQC NMR analysis of EtOAc-soluble products derived from wood after complete evaporation of EtOAc as described above.

Lignin-derived products obtained as EtOAc-soluble products from wood were analyzed by gas chromatography/mass spectrometry (GC/MS) on a GCMS-QP2010 Ultra instrument (Shimadzu Co., Kyoto, Japan) equipped with an Agilent CPSil 8CB column (length: 35 m, diameter: 0.25 mm) operating at 250 °C and the following temperature profile: 70 °C (holding time: 2 min), heating at 4 °C min^{-1} to 150 °C (1 min), heating at 10 °C min^{-1} to 310 °C (3 min). The carrier gas was H_2 (flow rate: 1.10 mL min^{-1}). The split ratio was 1/10 and the scan interval (35–500 m/z) was 0.3 s. Prior to each GC/MS trial, the lignin-derived products were subjected to a trimethylsilylation reaction performed in pyridine (100 μL), hexamethyldisilazane (150 μL) and trimethylchlorosilane (80 μL) at 60 °C for 30 min. 1,3,5-trimethylbenzene (Tokyo Kasei Kogyo Inc., Tokyo, Japan) was added as an internal standard. The molar yield of each monomer was calculated with the following equations as expressed on a phenylpropanoid (C9) aromatic unit basis. The average molecular weight (MW) of C9 units from lignin were reported to be 189.8 Da for softwood MWL ($C_9H_{8.3}O_{2.7}(OCH_3)_{0.97}$) and 212.3 Da for hardwood MWL ($C_9H_{8.3}O_{2.9}(OCH_3)_{1.58}$).[43] These values were chosen as representatives of the molecular weight of C9 units from lignins *in planta* and used in the present study. The molecular structures and abbreviations used for each monomeric product are summarized in Table 1.

$$\text{Molar yield(mol\%)} = \frac{\text{mass of monomer}}{\text{MW of monomer} \times n_{C9}} \times 100\%$$

$$n_{C_9}(\text{mol}) = \frac{\text{mass of lignin in sample}}{\text{MW of lignin } C_9 \text{ unit}}$$

The distribution of molecular weights in the EtOAc-soluble products was analyzed by gel permeation chromatography (GPC) on a Shimadzu LC-10A system equipped with a Shodex KF-801 column (exclusion limit: 1500 Da, polystyrene standard). The eluent was freshly distilled tetrahydrofuran (extra pure grade, Nacalai Tesque Inc., Kyoto, Japan) at a flow rate of 0.6 mL min^{-1}. The oven temperature was 40 °C and the UV detection wavelength was 280 nm.

Table 1 Chemical structures and abbreviations of lignin-derived monomers

Aromatic Type	Compound Name	Substituent (R)	Label
Syringol (S) 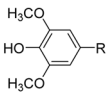	Dihydro sinapyl alcohol	-CH2-CH2-CH2-OH	S-DHA
	4-Propenyl syringol	-CH=CH-CH3	S-PrEn
	4-Propyl syringol	-CH2-CH2-CH3	S-Pr
	4-Ethyl syringol	-CH2-CH3	S-Et
	4-Methyl syringol	-CH3	S-Me
	Syringol	-H	S-H
Methoxycatechol (MC) 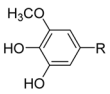	3-Methoxy-4-propyl catechol	-CH2-CH2-CH3	MC-Pr
	3-Methoxy-4-ethyl catechol	-CH2-CH3	MC-Et
	3-Methoxy-4-methyl catechol	-CH3	MC-Me
	3-Methoxy catechol	-H	MC-H
Guaiacol (G) 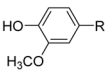	Dihydro coniferyl alcohol	-CH2-CH2-CH2-OH	G-DHA
	4-Propenyl guaiacol	-CH=CH-CH3	G-PrEn
	4-Propyl guaiacol	-CH2-CH2-CH3	G-Pr
	4-Ethyl guaiacol	-CH2-CH3	G-Et
	4-Methyl guaiacol	-CH3	G-Me
	Guaiacol	-H	G-H
Catechol (C) 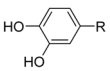	4-Propyl catechol	-CH2-CH2-CH3	C-Pr
	4-Ethyl catechol	-CH2-CH3	C-Et
	4-Methyl catechol	-CH3	C-Me
	Catechol	-H	C-H
Phenol (P) 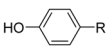	2,4-Dimethyl phenol	(2-CH3, 4-CH3)	P-2Me
	4-Propyl phenol	-CH2-CH2-CH3	P-Pr
	4-Ethyl phenol	-CH2-CH3	P-Et
	4-Methyl phenol	-CH3	P-Me
	Phenol	-H	P-H

Author Contributions

Alex Ikeda-Francisco: writing – original draft, methodology, investigation, formal analysis, data curation, visualization, conceptualization. Jiaqi Wang: data curation. Eiji Minami: writing – review and editing, visualization. Haruo Kawamoto: writing – review and editing, supervision, resources, project administration, methodology, funding acquisition, conceptualization.

Conflicts of interest

There are no conflicts to declare.

Data availability

The data underlying this study are available within the main text. The supporting data has been provided as supplementary information (SI). Supplementary information: Table S1, Fig. S1–

S12, NMR spectra of reaction products from the model compound experiments (Fig. S13–S20), representative GC chromatograms of gaseous products from Japanese beech (Fig. S21), GC calibration response factors (Table S2) and data regarding characterization of the commercial Pd/C catalyst (Fig. S22–S23). See DOI: https://doi.org/10.1039/d6ra00940a.

Acknowledgements

The present study was funded by the Japan Society for the Promotion of Science (Grant Number JP19H03019) and the JST-Mirai Program (Grant Number JPMJMI20E3), Japan.

References

1 IEA, Global Hydrogen Review2025, https://www.iea.org/reports/global-hydrogen-review-2025, 2025, (accessed 12 January 2026).
2 M. Zanon-Zotin, L. B. Baptista, R. Draeger, P. R. R. Rochedo, A. Szklo and R. Schaeffer, *Nat. Commun.*, 2024, **15**, 8050.
3 F. Kähler, M. Carus, O. Porc and C. Vom Berg, *Ind. Biotechnol.*, 2021, **17**, 245–258.
4 L. Wollensack, K. Budzinski, J. Backmann and C. Opin, *Green Sustain. Chem.*, 2022, **33**, 100586.
5 Y. Gao, M. Wang, A. Raheem, F. Wang, J. Wei, D. Xu, X. Song, W. Bao, A. Huang, S. Zhang and H. Zhang, *ACS Omega*, 2023, **8**, 31620–31631.
6 N. Ghavami, K. Özdenkçi, G. Salierno, M. Björklund-Sänkiaho and C. De Blasio, *Biomass Convers. Biorefin.*, 2023, **13**, 12367–12394.
7 J. A. Okolie, S. Nanda, A. K. Dalai, F. Berruti and J. A. Kozinski, *Renew. Sustain. Energy Rev.*, 2020, **119**, 109546.
8 Z. Liu, Y. Yang, Y. Chen, L. Yi, L. Guo, Y. Chao and H. Chen, *Biomass Bioenergy*, 2024, **190**, 107422.
9 A. V. Bridgwater, *Biomass Bioenergy*, 2012, **38**, 68–94.
10 H. Kawamoto, *J. Wood Sci.*, 2017, **63**, 117–132.
11 J. Wang, E. Minami and H. Kawamoto, *ChemistryOpen*, 2022, **11**, e202200104.
12 T. Kotake, H. Kawamoto and S. Saka, *J. Anal. Appl. Pyrolysis*, 2014, **105**, 309–316.
13 T. Kotake, H. Kawamoto and S. Saka, *J. Anal. Appl. Pyrolysis*, 2015, **113**, 57–64.
14 P. D. Vaidya and J. A. Lopez-Sanchez, *ChemistrySelect*, 2017, **2**, 6563–6576.
15 A. N. Joshi and P. D. Vaidya, *Int. J. Hydrogen Energy*, 2024, **49**, 117–137.
16 M. B. Valenzuela, C. W. Jones and P. K. Agrawal, *Energy Fuels*, 2006, **20**, 1744–1752.
17 X. Li, Y. Xu, K. Alorku, J. Wang and L. Ma, *Mol. Catal.*, 2023, **550**, 113551.
18 D. Vincent Sahayaraj, A. Lusi, A. J. Kohler, H. Bateni, H. Radhakrishnan, A. Saraeian, B. H. Shanks, X. Bai and J. P. Tessonnier, *Energy Environ. Sci.*, 2022, **16**, 97–112.
19 J. Wang, E. Minami and H. Kawamoto, *RSC Sustain.*, 2023, **1**, 1192–1199.
20 J. Wang, E. Minami and H. Kawamoto, *Green Chem.*, 2023, **25**, 2583–2595.
21 X. Ouyang, X. Huang, J. Zhu, M. D. Boot and E. J. M. Hensen, *ACS Sustain. Chem. Eng.*, 2019, **7**, 13764–13773.
22 Y. Liao, S.-F. Koelewijn, G. Van den Bossche, J. Van Aelst, S. Van den Bosch, T. Renders, K. Navare, T. Nicolaï, K. Van Aelst, M. Maesen, H. Matsushima, J. M. Thevelein, K. Van Acker, B. Lagrain, D. Verboekend and B. F. Sels, *Science*, 2020, **367**, 1385–1390.
23 Z. Liu, H. Li, X. Gao, X. Guo, S. Wang, Y. Fang and G. Song, *Nat. Commun.*, 2022, **13**, 4716.
24 J. Wang, E. Minami and H. Kawamoto, *J. Anal. Appl. Pyrolysis*, 2023, **170**, 105930.
25 Y. Wang, R. Eljamal, T. Nomura, E. Minami and H. Kawamoto, *J. Wood Sci.*, 2025, **71**, 39.
26 Y. Wang, D. Taira, R. Eljamal, T. Nomura, E. Minami and H. Kawamoto, *Ind. Crops Prod.*, 2025, **234**, 121599.
27 J. Wang, A. I. Francisco, E. Minami and H. Kawamoto, *Bioresour. Technol.*, 2025, **442**, 133676.
28 T. Nakamura, H. Kawamoto and S. Saka, *J. Anal. Appl. Pyrolysis*, 2008, **81**, 173–182.
29 H. Kawamoto, S. Horigoshi and S. Saka, *J. Wood Sci.*, 2007, **53**, 168–174.
30 T. Kotake, H. Kawamoto and S. Saka, *J. Anal. Appl. Pyrolysis*, 2013, **104**, 573–584.
31 T. Nakamura, H. Kawamoto and S. Saka, *J. Wood Chem. Technol.*, 2007, **27**, 121–133.
32 Y. Wang, W. Deng, B. Wang, Q. Zhang, X. Wan, Z. Tang, Y. Wang, C. Zhu, Z. Cao, G. Wang and H. Wan, *Nat. Commun.*, 2013, **4**, 2141.
33 W. Deng, P. Wang, B. Wang, Y. Wang, L. Yan, Y. Li, Q. Zhang, Z. Cao and Y. Wang, *Green Chem.*, 2018, **20**, 735–744.
34 V. Choudhary, S. H. Mushrif, C. Ho, A. Anderko, V. Nikolakis, N. S. Marinkovic, A. I. Frenkel, S. I. Sandler and D. G. Vlachos, *J. Am. Chem. Soc.*, 2013, **135**, 3997–4006.
35 S. Liu, X. Cheng, S. Sun, Y. Chen, B. Bian, Y. Liu, L. Tong, H. Yu, Y. Ni and S. Yu, *ACS Omega*, 2021, **6**, 15940–15947.
36 O. Bobleter, R. Niesner and M. Röhr, *J. Appl. Polym. Sci.*, 1976, **20**, 2083–2093.
37 S. Saka and T. Ueno, *Cellulose*, 1999, **6**, 177–191.
38 T. Adschiri, S. Hirose, R. Malaluan and K. Arai, *J. Chem. Eng. Jpn.*, 1993, **26**, 676–680.
39 M. Asmadi, H. Kawamoto and S. Saka, *J. Anal. Appl. Pyrolysis*, 2017, **124**, 523–535.
40 A. Bjorkman, *Sven. Papperstidn.*, 1956, **59**, 477–485.
41 B. Qi, L. Di, W. Xu and X. Zhang, *J. Mater. Chem. A*, 2014, **2**, 11885–11890.
42 E. Minami, T. Miyamoto and H. Kawamoto, *Hydrogen.*, 2022, **3**, 333–347.
43 C. W. Dence and S. Y. Lin, in: *Methods in Lignin Chemistry*, Springer Berlin Heidelberg, Berlin, Heidelberg, 1992, pp. 3–19.